MUPUS – A THERMAL AND MECHANICAL PROPERTIES PROBE FOR THE ROSETTA LANDER PHILAE

TILMAN SPOHN[1,2,*], KARSTEN SEIFERLIN[3], AXEL HAGERMANN[4], JÖRG KNOLLENBERG[2], ANDREW J. BALL[4], MAREK BANASZKIEWICZ[5], JOHANNES BENKHOFF[2,7], STANISLAW GADOMSKI[5], WOJCIECH GREGORCZYK[8], JERZY GRYGORCZUK[5], MAREK HLOND[5], GÜNTER KARGL[6], EKKEHARD KÜHRT[2], NORBERT KÖMLE[6], JACEK KRASOWSKI[5], WOJCIECH MARCZEWSKI[5] and JOHN C. ZARNECKI[4]

[1] *Institut für Planetologie, Westfälische Wilhelms Universität, Münster, Germany,*
[2] *Institut für Planetenforschung, Deutsches Zentrum für Luft- und Raumfahrt, Berlin, Germany*
[3] *Physikalisches Insitut, Universität Bern, Bern, Switzerland*
[4] *Planetary and Space Science Research Institute, CEPSAR, The Open University, Milton Keynes, UK*
[5] *Space Research Centre, Warsaw, Poland*
[6] *Institut für Weltraumforschung, Österreichische Akademie der Wissenschaften, Graz, Austria*
[7] *European Space Technology Centre, ESA, Noordwijk, The Netherlands*
[8] *Telecommunication Institute, PIT, Warsaw, Poland*
*(*Author for correspondence: E-mail: Tilman.Spohn@dlr.de)*

(Received 28 February 2006; Accepted in final form 11 October 2006)

Abstract. MUPUS, the **mu**lti **pu**rpose **s**ensor package onboard the Rosetta lander PHILAE, will measure the energy balance and the physical parameters in the near-surface layers – up to about 30 cm depth- of the nucleus of Rosetta's target comet Churyumov-Gerasimenko. Moreover it will monitor changes in these parameters over time as the comet approaches the sun. Among the parameters studied are the density, the porosity, cohesion, the thermal diffusivity and conductivity, and temperature. The data should increase our knowledge of how comets work, and how the coma gases form. The data may also be used to constrain the microstructure of the nucleus material. Changes with time of physical properties will reveal timescales and possibly the nature of processes that modify the material close to the surface. Thereby, the data will indicate how pristine cometary matter sampled and analysed by other experiments on PHILAE really is.

Keywords: rosetta, comets, surface, heat flow

1. Introduction and Scientific Goals

Rosetta was sucessfully launched on 2 March 2004 and is expected to start its rendevous with Comet Churyumov-Gerasimenko in May 2014. The Rosetta Lander PHILAE will be the first spacecraft to make a soft landing on a comet nucleus. Scientific observations are to be carried out for a minimum of one week, but might continue for several months as the comet approaches perihelion. Rosetta's target comet Churyumov-Gerasimenko has a period of ∼6.6 years. its nucleus, with an estimated size of 3×5 km, is expected to have a rotation period of approx 12 hours.

Space Science Reviews (2007) 128: 339–362
DOI: 10.1007/s11214-006-9081-2

The physics of comets involves the production of the coma by the sublimation of ices at or close to the surface of the nucleus. The rates of production of coma gases depend on the energy balance at the surface and in a boundary layer underneath the surface into which heat is transferred by conduction and vapour transport. The surface energy balance is

$$\sum R_i H_i = S - \varepsilon\sigma T^4 - (q + q_v) \tag{1}$$

where R_i are the sublimation rates of the coma gases (species i), H_i is the enthalpy of sublimation of species i (approx. $2.8 \times 10^6 \mathrm{Jkg}^{-1}$ for water ice), S is the insolation corrected for the surface albedo, ε is the surface emissivity (slightly less than 1.0 for a 'dark' comet), σ the Stefan-Boltzmann constant, T is temperature and q and q_v are the conductive heat flux and the heat flow associated with the vapour flow into or out of the interior, respectively. Temperatures at a dust-covered surface can exceed the temperature of a sublimating water ice surface ($\sim$200 K) by more than 100 K near 1AU. The vapour flux into the interior is driven by the gradient in vapour density that forms in response to the temperature gradient during cometary day time. The gas flow is likely to be in the Knudsen regime. During night time the flow may be reversed.

The energy balance in the porous interior of the nucleus reads

$$\rho c \frac{\partial T}{\partial t} + \sum H_i \frac{\partial \rho_i}{\partial t} = -\nabla \cdot \vec{q} - \sum \rho_i c_i \vec{u}_i \cdot \nabla T \tag{2}$$

where ρ and c are the density and specific heat of the nucleus ice, ρ_i, c_i, and u_i are the densities, specific heats (at constant volume) and flow velocity of vapour species i in the interior. Since the vapour pressures are functions of temperature, the ratio between the two heat transport terms on the right-hand-side (RHS) of (2) depends on the temperature, the enthalpy of sublimation and on the thermal diffusivity and permeability of the ice. The thermal properties of the ice are not precisely known. Depending on pore volume and structure in the ice, thermal conductivity could be 2 or more orders of magnitude lower than solid ice, i.e. 568/T W $\mathrm{m}^{-1}\mathrm{K}^{-1}$ (Klinger, 1981), so that the vapour could contribute considerably to the total energy transport. Smoluchowski (1982) was the first to point to the importance of heat transfer via the vapour phase. It has been demonstrated experimentally through the KOSI (comet simulation) experiments (e.g., Grün *et al.*, 1991) that heat transfer via vapour was important at temperatures above about 200 K for water ice (Spohn and Benkhoff, 1990; Steiner, 1990; Benkhoff and Spohn, 1991; Espinasse, 1991; Steiner and Kömle, 1991; Steiner *et al.*, 1991; Benkhoff *et al.* 1995). Spohn and Benkhoff (1990) have outlined a porous medium heat and mass transfer theory to describe the effects. Benkhoff and Huebner (1995) and Huebner and Benkhoff (1997,1999) expanded the model and applied it to cometary nuclei.

MUPUS ('Multi-Purpose Sensors for Surface and Sub-Surface Science') originated from the proposal to the then RoLand comet lander by Spohn *et al.* (1995),

with a related experiment ('SuSI') also having been proposed for the (ultimately cancelled) Champollion lander (Benkhoff *et al*., 1995). The central part of MUPUS is a thermal probe that, after insertion into the regolith of the comet nucleus up to a depth of 32 cm, aims to measure both the temperature profile underneath the surface and the thermal diffusivity and conductivity profiles. The thermal diffusivity and conductivity will be derived from the time rates of change of sensor temperatures during active heating cycles. In addition, MUPUS will measure the surface temperature and the mechanical strength of the nucleus material. The temperatures and the thermal transport parameters will be measured regularly over the life time of the lander. The mechanical strength of the material will be derived from the energy spent per unit distance penetrated during the hammered insertion. Profiles of penetration resistance will also be derived from MUPUS accelerometry measurements in each of the lander's two harpoon anchors. The anchors also contain MUPUS temperature sensors.

In doing these measurements, MUPUS can contribute to an assessment of the energy balance of the comet nucleus and the physical properties of its material. Since the thermal conductivity and diffusivity are strong functions of the structure of the porous ice and the degree to which it has been sintered (Seiferlin *et al*., 1995), MUPUS can constrain the microstructure and the degree to which the comet material has been thermally altered. MUPUS will thus predict at what depth pristine material can be expected. This is important for characterising the context of the samples extracted by the drill, as well as for our understanding of the thermophysics of cometary activity. The scientific objectives of MUPUS are summarised as follows:

– To understand the properties and layering of the near-surface matter as these evolve with time as the comet nucleus spins and approaches the Sun.
– To understand the energy balance at the surface and its variation with time and depth.
– To understand the mass flow at the surface and its evolution with time.
– To provide ground truth for thermal mapping from the Orbiter, and to support other instruments on the Rosetta Lander (e.g. SESAME-CASSE)."

2. Instrument Description

The MUPUS package consists of three major parts, the penetrator MUPUS PEN with ist subsystems, the radiometer MUPUS TM, and the anchor sensors MUPUS ANC. Their positions on the lander are coloured red in Figure 1. The MUPUS main electronics are integrated into the Common Electronics Box on the lander, together with the main electronics of other experiments and lander subsystems.

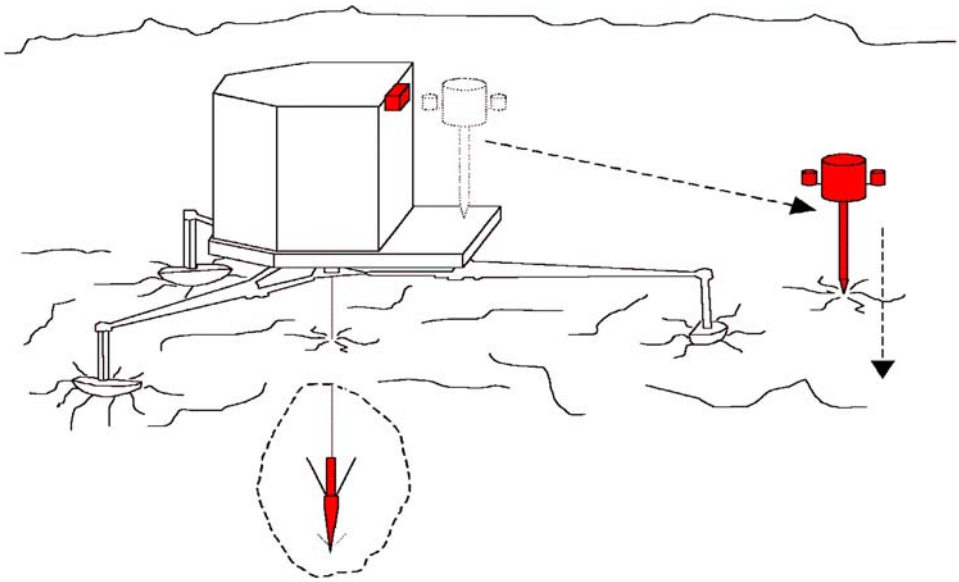

Figure 1. MUPUS instrument package configuration overview. The penetrator is placed on the surface away from the lander by a deployment arm (not shown). Both anchors of the lander harbour a temperature sensor (ANC-T) and an accelerometer (ANC-M). The 4-channel IR sensor TM is mounted near the top of the lander housing. The penetrator is equipped with a depth sensor (PEN-M), thermal sensors that measure the temperature profile (TP) and a thermal diffusivity / conductivity profile (THC). The hammering device and the front-end electronics are mounted in the housing (thick cylinder) on top of the penetrator tube (thin cylinder).

2.1. The Penetrator MUPUS PEN

The main part and the most complex instrument in the MUPUS experiment suite is the thermal probe **MUPUS PEN** (Figure 2). A fibre compound tube with a metal tip will be inserted into the ground about one meter away from the lander by a deployment device and a hammer mechanism (Seiferlin *et al.*, 2002). The hammer mechanism is accommodated together with heated front end electronics in a gold plated cylinder housing at the top of the penetrator and will remain above the surface. The total length of the probe is restricted by the vertical height of the lander on the balcony of which MUPUS PEN was required to fit. The hammer and electronics housing is about 10 cm high, leaving 33 cm for the tube and 3 cm for the tip. The length of the tube is several times the thermal skin depth for rotation rates of the nucleus between 10 and 100 h and thermal conductivities less than that of compact ice. We consider a skin depth of only a few cm as most likely.

Until its descope in mid-2001, MUPUS PEN also incorporated a gamma ray densitometer (Ball *et al.*, 2001). It was designed to measure the attenuation of gamma rays emitted by a ^{137}Cs source in the tip of the penetrator. During penetration the

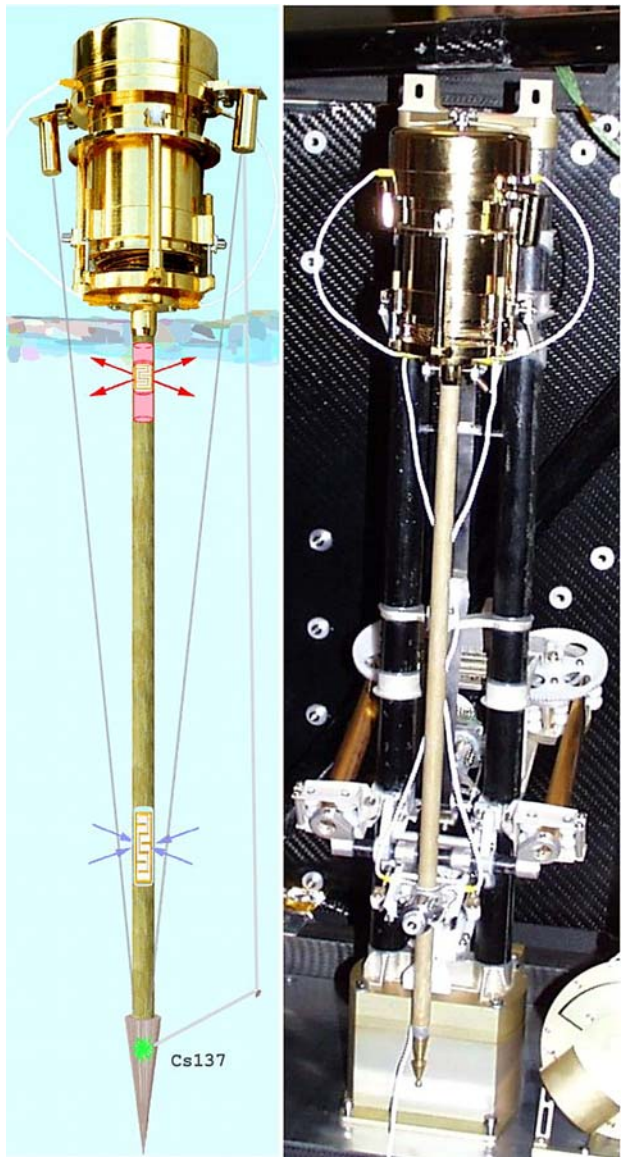

Figure 2. MUPUS PEN: The right image shows the MUPUS PEN, mounted on the lander (launch and cruise phase configuration). A stepper motor (lower centre, between the two black support tubes) will uncoil two metal profiles (brass-coloured) from their stored position on two spools (left and right of the stepper motor) and thus deploy the penetrator to a distance of about 1 m from the lander. A hammer (in the gold-plated cylinder on top) will insert the probe (thin, brownish tube) into the regolith. The tube carries 16 thermal sensors that can be used to measure the temperature. These sensors can also be used to heat the surrounding comet regolith (2 such sensors are shown in the left panel) for a measurement of the thermal conductivity. A densitometer photon source and two densitometer detectors (top, next to the hammer housing) were planned to be integrated (left image). The densitometer had to be descoped because of the lack of funding.

changing flux of transmitted gamma rays would have been measured by two semiconductor detectors mounted on opposite sides of the front-end electronics. The sensor was descoped because of technical problems arising ultimately from funding difficulties in the early stages of the project. Unfortunately, the vertical profile of bulk density will now have to be inferred by other means. For example, a bulk density profile might be retrievable via microstructural models of the sub-surface material, constrained by other physical properties measurements as well as compositional information. Such measurements include: mechanical properties measurements made by the MUPUS thermal probe during hammering, anchor deployment and sampling drill operation; thermal diffusivity measurements made by the MUPUS thermal probe; permittivity measurements made by the SESAME-PP experiment; acoustic wave propagation measurements made by the SESAME-CASSE experiment (Seidensticker *et al*., this volume); surface thermal inertia measurements made nearby by MUPUS-TM, and compositional measurements made by the Philae geochemical experiments. Larger-scale bulk density can also be assessed by the orbiter radio science experiment and by the CONSERT radio transmission tomography experiment (Kofman *et al*., this issue).

2.1.1. *The Thermal Probe*

The tube has a radius of 10 mm and a wall thickness of 1 mm. The mantle of the hollow tube is made of cyanato-ester with fibreglass, which has a thermal conductivity of 0.5 $\mathrm{Wm^{-1}K^{-1}}$. This material choice provides a good compromise between the structural requirement of being stiff enough to penetrate the surface, and the thermal requirement to minimize vertical heat flow along the probe. A more important factor for this heat pipe effect is, however, not the probe itself but the sensors and their conductors which are made of Titanium and copper, respectively. Though they are only a few micrometres thick, their total conductance is about twice that of the fibre compound tube. The heat pipe effect of the probe can be illustrated by a comparison of the total conductance of the probe with estimates of that of the cometary material that occupied the volume within the tube before insertion. For a thermal conductivity of the replaced porous cometary material of 0.1 $\mathrm{Wm^{-1}K^{-1}}$ the probe conducts about 5 times as much heat as the material it replaced. In addition, the thermal effect of the zone of compacted material around the inserted probe needs to be taken into account.

The effect of a thermal 'short circuit' through the probe is minimised by using a thin, hollow probe of a low-conductivity material, but significant enough that it needs to taken into account in the data analysis. However, remaining perturbations can be reduced by an inversion-type data evaluation method that was developed by the MUPUS team (Hagermann, 1999; Hagermann and Spohn, 1999). This method makes use of the damping and lagging effect which temperature signals from the surface experience as they penetrate to greater depths. More details about this method can be found in the appendix.

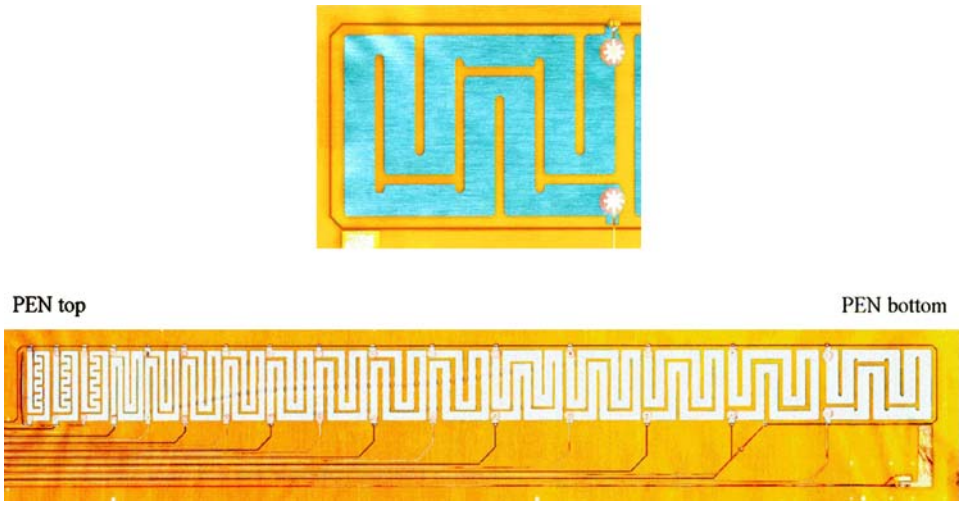

Figure 3. A new type of thermal sensor has been developed by the MUPUS team. A 20 μm thin layer of titanium on a Kapton substrate is used to measure the temperature (electrical resistance is proportional to the temperature). The same titanium cell can be actively heated in order to perform thermal diffusivity and conductivity measurements (upper panel). 16 such cells and all required electrical connections (thin lines) are laser-sputtered on one Kapton sheet (lower panel). The cell dimensions grow from top (left in image) to bottom. The Kapton sheet is rolled and glued to the inner tube wall of MUPUS PEN.

2.1.2. *The Thermal Sensors*

The PEN tube carries a Kapton sheet that is glued to its inner wall onto which the thermistors are vapour deposited. The technology used for manufacturing the thermal sensors was developed by the MUPUS team for the experiment. It is described in Gregorczyk *et al.* (1999).

The Kapton sheet is glued to the inner wall of the tube in order to protect the thermal sensors from mechanical strain upon insertion. There are sixteen meander-shaped titanium sensors with temperature-dependent electrical resistance (see Figure 3). The number of sensors matches the number of independent data channels of the electronics. The depth intervals covered by these sensors increase from the top to the tip of the tube, from 1 cm to 4 cm length. This configuration has been chosen in order to allow a denser coverage of the thermal profile near the surface where the temperature gradient is expected to be steeper than at greater depth. The resistance of the titanium is a function of temperature similar to the temperature dependence of the resistance of PT100 type sensors. PT100 sensors and their use for temperature measurements are standardized under the IEC 751 norm, its European counterpart EN 60751 and the German DIN 60751.

The temperature dependence is given by

$$R(T) = R_0(1 - s_1 \cdot \Delta T + s_2 \cdot \Delta T^2) \tag{3}$$

where R_0 is a reference resistance of 100 Ohm at a reference temperature of 275.73 K, ΔT is the temperature difference to the reference temperature. For a PT100 and other platin-based sensors, s_1 in eq. 3 is 3.9083×10^{-3} K^{-1}, and $s_2 = -5.775 \times 10^{-7}$ K^{-2}.

The linear coefficient s_1 for other bulk metals is typically in the order of 4×10^{-3} K^{-1}, while s_2 is typically two or more orders of magnitude smaller. The relation holds for a temperature interval of 110 K to 375 K. For the MUPUS-type Titanium sensors, s_1 and s_2 have to be determined individually for each sensor, because tabulated values for bulk metals cannot be applied to thin films of vacuum-deposited metal. s_1 was found to be about 2×10^{-3} K^{-1} with small variations between individual sensors, which is about half the value of that for PT100. After vacuum-deposition on the Kapton sheet, the sensors have been tempered and cured. This procedure has been repeated after integration of the Kapton sheet into the hollow tube. The long-term stability of the sensor's characteristics is unknown. In-flight calibration will be required.

The 16 sensors thus allow measuring a temperature profile that extends over the length of the tube (32 cm). Because of the small mass of the sensors the reaction time of the sensors to changes in temperature is small, typically a few seconds. The specific thermal timescale for a sensor being separated from the medium by 1 mm (i.e. the thickness of the probe wall) of a material with a thermal diffusivity of about 10^{-6} m^{2}s^{-1} is one second. The surface (proportional to heat flux) to volume (proportional to total heat capacity) ratio of a MUPUS-type sensor is 100 times better than that for a conventional ceramics-sealed PT100, and reacts to changes in temperature faster by about the same factor. The sensitivity of the bare sensors is slightly worse than that of PT100 standard sensors because of the difference in s_1 in Equation (3). The effective resolution of the flight instrument is limited by the performance of the 16 bit AD converter to about 12 meaningful bits, covering about 200 K, which corresponds to about 0.05 K (see also Marczewski *et al.*, 2004). The temperatures are measured by applying a constant current of 20 mA and measuring the voltage drop across the resistors. All PEN sensors are connected to the current source through one shared conductor and individual sensor wires inside the probe structure, and two external PEN cables. The number of wires is limited to 18 in order to minimize undesired heat losses along the cables. Several options are available for the measurement sequence, but a default operation is defined for long term operations, consisting of a temperature scan every 20 sec.

2.1.3. *Expected Performance*

Initial tests of the probe performance were obtained by heating individual sensors in vacuum with background temperatures between -160 C and -100°C as well as under ambient conditions with the PEN probe immersed in different media. These tests showed that the influence of the heating on the neighbouring sensors is moderate and that mainly the immediate neighbours are affected. The temperature increase in immediately adjacent sensors will depend on the thermal conductivity

of the nucleus surface layer but is expected to be relatively small. Under worst conditions in vacuum we measured a temperature rise of the neighbour sensor by about 50% of the temperature of the heated sensor depending to some extent on the ambient temperature. In solid ice the increase was 5%, in snow and sand 10–15% and in a Teflon cylinder with a thermal conductivity of 0.25 W/m K about 10%. Additional tests with a model of the MUPUS penetrator in terrestrial soil showed that the penetrator was more sensitive to weak energy fluxes than the commonly used method of heat flux plates (Marczewski *et al*., 2004). These authors have reported on a series of test experiments with the MUPUS thermal probe.

In order to demonstrate and illustrate the performance of MUPUS PEN measuring the temperature profile of the uppermost layers of a comet, we studied two different data sets that are related to cometary thermal evolution, and come from two quite different sources:

1. In recent years, the International Space Science Institute ISSI, located in Bern, gathered comet modellers (one of them was J. Benkhoff, co-author of this paper) in a group and invited this group several times to workshops. One goal of this 4-year program, coordinated by W. Huebner, was to compare individual model codes, improve them and finally develop a set of standard thermophysical comet models. The used model code is a 1-dimensional, multi-component (e.g., water, CO) finite difference code which solves a set of coupled mass- and heat diffusion differential equation, thus including heat transport by the vapour phase. We selected a model comet with the following key parameters: (a) A spherical model comet in an orbit of the Rosetta target comet P/Wirtanen, (b) the spin axis is assumed to be perpendicular to the orbital plane, (c) porosity is simulated by a pipe network (pore radius 10mm), (d) the nucleus consists of water ice, several minor volatile components, and dust, (e) molecular flux in the pores, (f) low heat conduction (Hertz factor 0.001).
   The model calculations were carried out as follows: a homogeneously mixed body at a constant initial temperature (T = 20K) and a constant mass density distribution is considered. Due to heating of the body and sublimation of the volatile components, the initially homogeneous body differentiates into a multi-layer body (if it contains more than one volatile component), where the deepest layer has the original composition. The subsurface temperatures are calculated every 15 Minutes for several orbits. The underlying model is described in Benkhoff (2002) and Prialnik *et al*. (2004).
2. From ca. 1987 to 1992, the German Research Foundation (DFG) sponsored a research program in which several German and International teams cooperated in oder to simulate comets, (see Grün *et al*., 1991, for example) or at least some physical processes with relevance to comets, in a large space simulator – basically a vacuum chamber equipped with a LN2 cooling facility and an arrangement of Xenon lamps to simulate solar insolation. In each of the KOSI ("Kometen-Simulation" = Comet Simulation) experiments, a sample of porous ice-dust

mixtures was filled into a sample container of typically 30 cm diameter and 15 cm depth, then cooled down in vacuum and finally exposed to artifical sunlight. We (Benkhoff, Spohn and Seiferlin) were responsible for the thermal measurements during these experiments. The selected KOSI-9 test was special in one respect: there were 3 subsequent insolation periods of more or less similar intensity profile (the first one a bit shorter but all with the same intensity profile) and a total experiment duration of about 70 h, in order to simulate natural day/night cycles. Differences between the temperature profiles for the 3 phases can be explained by texture modification like sintering and recrystallization of water ice, which would be more effective in warm layers. This KOSI 9 experiment was described by Seiferlin *et al*. (1995).

Temperature profiles from both sources were processed in the same way to simulate a measurement done with MUPUS:

1. The temperature profiles, as they were available, contained fewer data points in z-direction than MUPUS would measure. The profiles were therefore projected onto an array of sufficient length, and gaps between existing data points were filled by a polynomial fit. In the time domain, an artificial equidistant data set with sufficient resolution was generated by interpolating between existing time steps (i.e. subsequent data points).
2. Because the individual MUPUS sensors are between 10 and 40 mm long, they record the average temperature along their length. The fitted temperature profile obtained in step 1 was projected onto the geometry of the MUPUS sensors in such a way that each sensor was assigned a temperature equivalent to the average temperature of the stretch covered by the sensor considered. After this step, the temperature profile consisted of 16 temperature values, just as they would be recorded by MUPUS.
3. In this step, the quality of the data was degraded and limited to 10 bit resolution, which is slightly less than provided by the MUPUS flight electronics.
4. Moderate random noise was then added to simulate random errors such as may be caused by varying thermal contact to the medium, calibration uncertainties, electromagnetic noise etc.
5. The temperature profile as a function of time was then converted into a colour coded image. The colour palette contains only 256 colours corresponding to 8 bit resolution. Thus, the resolution of the data as represented by the colour maps is degraded in comparison with the expected results from MUPUS. The simulated time step is 5 minutes according to the the nominal measurement cycle of MUPUS.

Figure 4 shows a simulated measurement of the comet temperature history as was proposed by the ISSI working group. Figure 5 shows the KOSI 9 data set. Because the KOSI 9 record covered only 15 cm depth, the simulated MUPUS measurement was also truncated at 15 cm. The results suggest that if the ISSI and the KOSI results

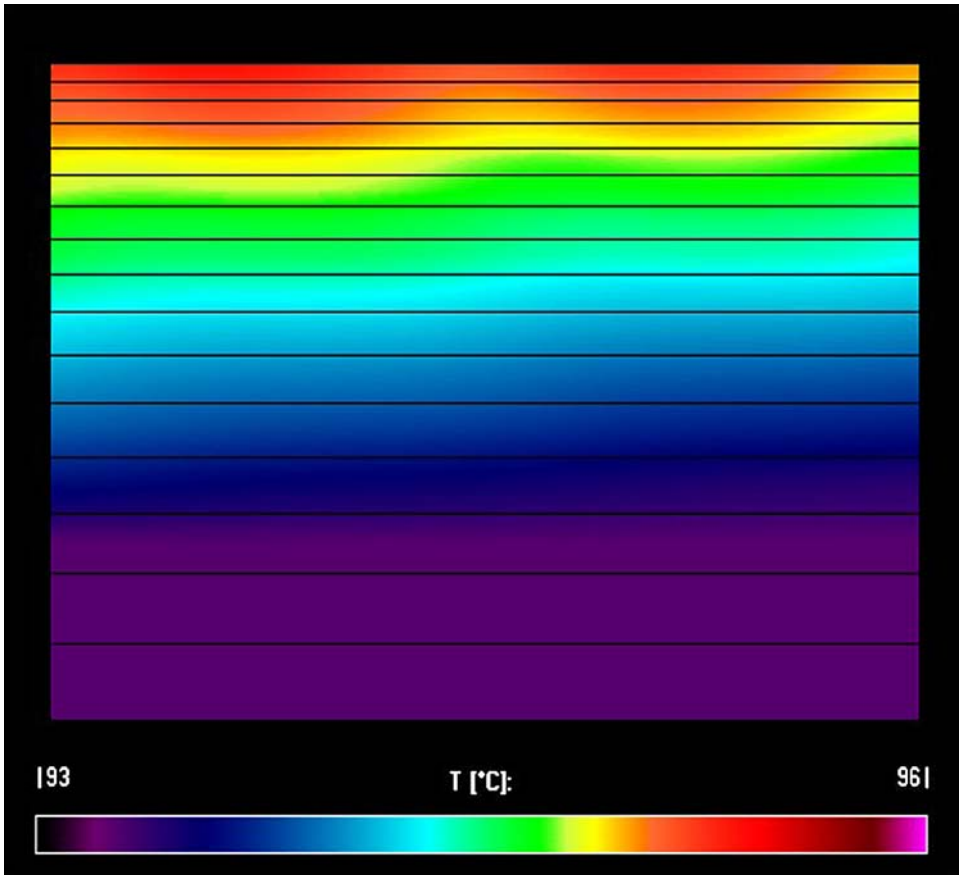

Figure 4. Simulated measurement with MUPUS. Temperatures are color coded in Kelvin. Time is horizontal, depth is vertical. The time step (i.e. measurement interval and pixel resolution in the image) is 5 minutes. The maximum depth is 32 cm. Black horizontal lines indicate sensor edges. The temperature data processed for this image were taken from a numerical model of comet nucleus temperatures developed in the framework of an ISSI working group, and were provided by J. Benkhoff. See text for further description.

are representative of the near surface temperature profiles in a cometary nucleus, the MUPUS probe should be suitable to record it. The total penetration depth and the number and spacing of sensors seems appropriate and, considering the limited resources on the Rosetta Lander PHILAE, satisfactory.

2.1.4. *Transient Thermal Properties Measurements*

The titanium resistor cells may also be heated by applying electrical power to them of up to 1 W at 12 V. The temperature increase caused by the heating is a function of the known power and the thermal diffusivity (resp. conductivity) of the material that surrounds the heated cell(s). In a typical measuring cycle, the heating is applied for a

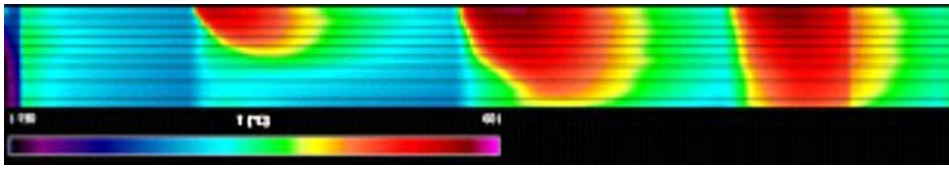

Figure 5. Simulated measurement with MUPUS. Temperatures are color coded in Kelvin. Time is horizontal, depth is vertical. The time step (i.e. measurement interval and pixel resolution in the image) is 5 minutes, total duration is 70 hours. The maximum depth is 15 cm. Black horizontal lines indicate sensor edges. The temperature data processed for this image were taken from the results of the KOSI 9 experiment (see text for further detail). Three day/night cycles are visible. The discontinuity at the afternoon of the third day is caused by a data gap in the original data set.

given time interval (5 minutes under standard conditions) and is then interrupted for a temperature measurement for a few milliseconds. The temperature measurement thus affects the heating only insignificantly. After switching off the heating power, the temperature relaxation can additionally be measured.

The heating power is controlled by the filling ratio of the pulses, varying from zero to the maximal available power (approx. 1 W) with 12-bit resolution. Under standard operational conditions, heating will use up to 1/4th of the maximal available power (approx. 0.2–0.3 W). Heating will be applied to one or more sensors simultaneously. For a measuring a conductivity depth profile, heating will be applied consecutively to sensors with increasing depth. The heating and the associated temperature measurements can be repeated every hour.

The evaluation of the data to obtain diffusivity and conductivity profiles is not straightforward, but Banaszkiewicz *et al.* (1997) have derived appropriate mathematical tools.

2.1.5. *The Hammer*

The difficult task to emplace a sub-surface probe into a medium of unknown hardness (but not harder than ca. 2 MPa) is performed by a mechanical hammer, especially designed for MUPUS. The hammer works like a mechanical diode. A conventional 22 μF capacitor is charged to several 100 V. The stored electrical energy is discharged through a coil that generates a strong magnetic field. A small mass (30 g) is accelerated by the magnetic field into the opening inside the coil and hits the penetrator tube with its maximum speed of $\sim$8 m/s, thus causing a powerful hammer stroke onto the tube. The friction exerted on the tip and the tube and some weak force extended by the deployment device take most of the rebound following the hammer stroke. Together, hammer stroke and rebound absorption cause a net forward movement of the penetrator into the comet nucleus regolith. Both the tube and the hammer mass are connected by weak springs to the hammer housing. These springs act to bring both back to their starting positions and prepare the motor for

the next hammer stroke. The energy of the hammer strokes can be adjusted to the requirements set by the hardness of the nucleus material .

The probe also includes a sensor (PEN-M) to monitor the vertical displacement of the probe as it is inserted. It starts close to the tip and slides up the probe; the displacement is sensed electrically in the manner of a potentiometer. The assembly carrying the displacement sensor also houses an electromagnet to hold the penetrator and one of the electrodes of the SESAME-PP (Permittivity Probe) experiment (Seidensticker *et al*., this issue).

Compared to alternative insertion methods, e.g. a pyro, the mechanism has several advantages:

- the total energy is only limited by the power supply offered by the hosting spacecraft, while a pyro has a maximum stored energy defined at design time,
- insertion is done in small steps and may be interrupted to take measurements once a given depth is reached,
- the advancement of the penetrator is small enough such that the insertion efficiency (depth reached per dissipated electrical energy) can be measured. From these data a cohesion profile of the penetrated layers can be derived.

Whenever erosion of the cometary surface material re-exposes parts of the penetrator, the hammer can be restarted to compensate for the material loss at the top by inserting the penetrator accordingly. The expected surface erosion may well reach 1 m per comet orbit. This is about 3 times the total length of the penetrator tube.

2.1.6. *Front-end electronics*

To keep the thermal losses of the lander small and to reduce the harness between the penetrator and the lander, a front-end electronics package has been included in the hammer housing. The front-end electronics package communicates with the electronics on board the lander via digital signals only, using a serial interface. The cable connection between the lander and the front-end electronics is routed through the central rotation axis of the lander, below the baseplate. This configuration ensures that the lander can rotate after PEN deployment without being locked by a direct, tense cable connection to the balcony, for example. The design of the front-end electronics proved to be very demanding, since it has to operate in a low temperature environment, while the small size and mass of the housing make an effective thermal design difficult. Figure 6 shows the layout of the MUPUS electronics. A detailed thermal model of the Front-End electronics can be found in Seweryn *et al*. (2005).

2.1.7. *The Deployment Device*

Measuring the nucleus energy balance in the near-surface layers requires a thermal probe that will be placed far enough away from the lander's shadow. This requirement made it necessary to design and develop a complex mechanical deployment device for the MUPUS PEN. The deployment device (compare Figures 1, 2 and

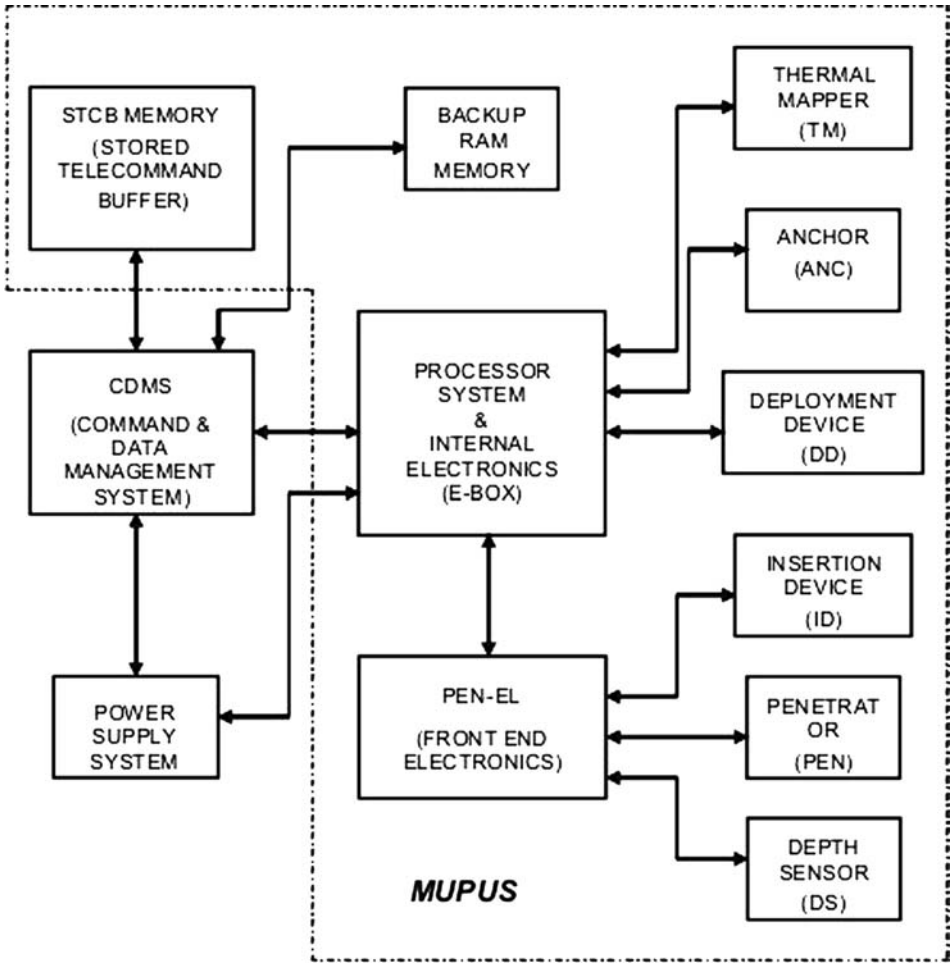

Figure 6. Layout of the MUPUS electronics and its integration into the Philae lander. MUPUS's main electronics components are the internal electronic box and the PEN front-end electronics.

7) will place the penetrator normal to the ground about 1 m away from the lander. The value of 1 m was determined from model calculations that investigated the subsurface temperature field underneath a lander on a slowly spinning comet nucleus. An example of the results is shown in Figure 8. Because the lander is intended to rotate after MUPUS PEN deployment, the deployment device must be separated from the penetrator and retracted after deployment. A cable then provides communications and power to the penetrator while the lander can rotate freely. The design solution solves both problems efficiently: two spools hold one metal strip each that is coiled flat in its stored configuration. For deployment, a stepper motor pulls these approximately one meter long metal profiles forward from the spool

Figure 7. The MUPUS PEN and deployment device during a deployment test.

and the metal profiles attain their naturally bent shape. Their C-like cross section provides sufficient stiffness to hold the penetrator in the low-gravity environment and supports the PEN driving, which is especially important at the initial insertion phase. After PEN insertion, the PEN is released from the deployment device and the metal strips retracted onto the spools.

2.2. The Thermal Mapper

The MUPUS Thermal Mapper **TM** (see Figure 9) is an infrared radiometer that consists of a set of 4 IR (thermopile-type) sensors designed to measure the brightness temperature at the very surface, averaged over its field of view. In its normal mode, MUPUS TM will have the MUPUS penetrator in the center of its field of view, thereby adding an important data point to the temperature profile. Fragile, fluffy layers such as a dust mantle on the cometary surface with low thermal conductivity may cause a strong temperature gradient with depth and a significant temperature drop within a few mm below the surface. These first few mm cannot be resolved with the thermal sensors on MUPUS PEN even where the sensors are closely spaced. In

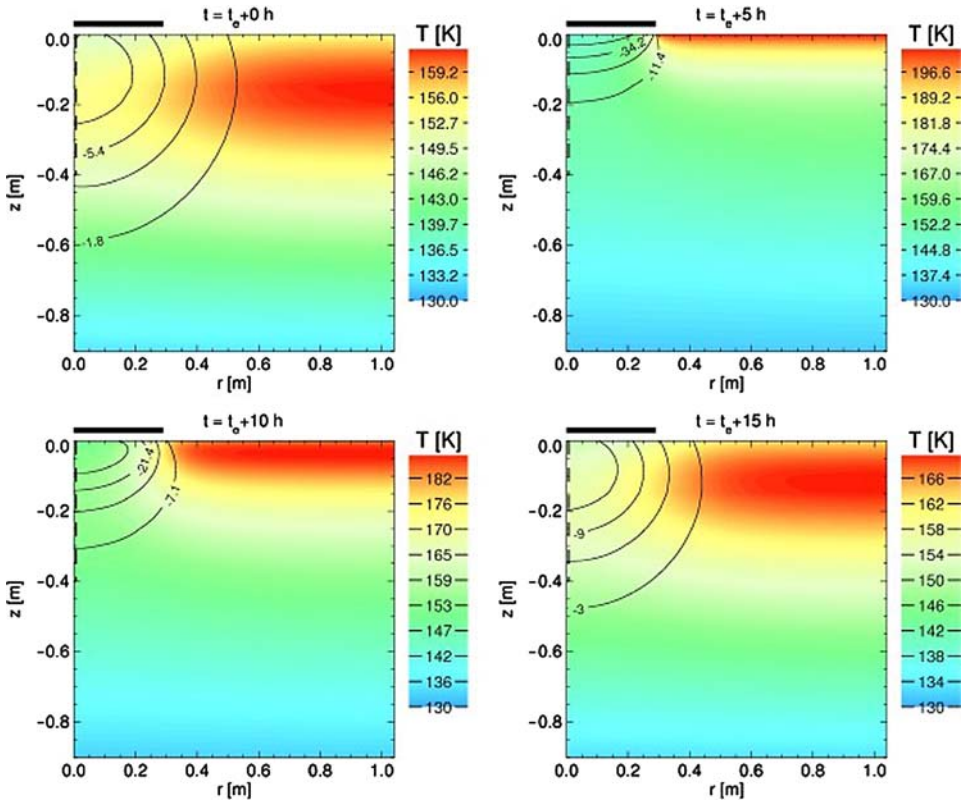

Figure 8. Temperature field as a function of radius and depth underneath a circular lander on a slowly rotating nucleus (20h period) made of porous water ice whose matrix is 20 times less heat conductive than compact ice. Representing a worst case, this model shows that the temperature profile underneath or even near the lander is not representative of the undisturbed profile. T_e corresponds to sunrise. Solid isotherms indicate the deviation in Kelvin from the temperature profile without a lander shadow.

addition to the surface temperature, a direct estimate of the thermal conductivity of the nucleus surface layer can be derived from the temperature measurements of TM and the uppermost temperature sensor of the penetrator. Furthermore, the thermal inertia of the nucleus surface at the landing site can be determined from an analysis of the TM data.

2.3. Anchor Sensors

The third component of MUPUS is the set of sensors implemented in Philae's two anchors MUPUS ANC (compare Figure 1). The anchors have been described by Thiel *et al.* (2001, 2003). Two types of sensors have been implemented:

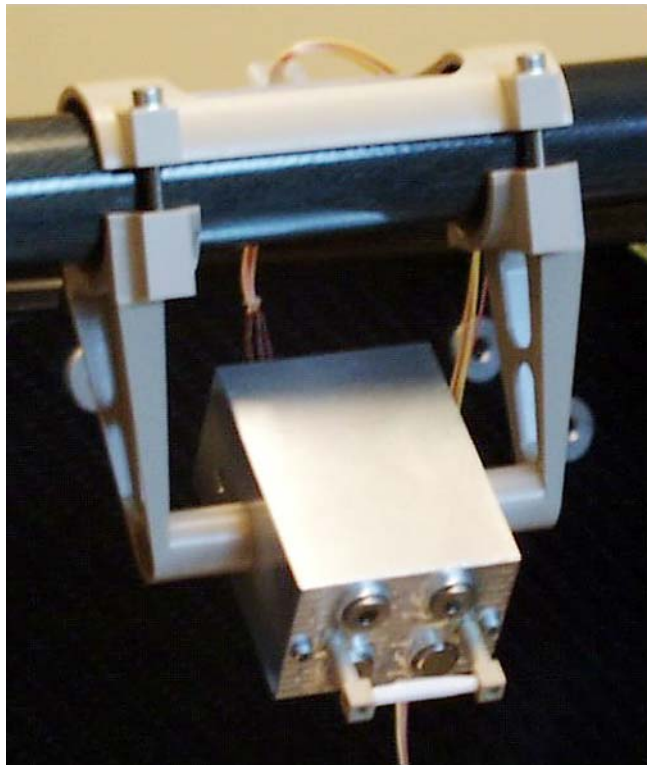

Figure 9. MUPUS TM: 4 thermopile-type IR sensors and a small front-end electronics package are mounted in a small housing fixed to a diagonal strut above the lander balcony. The box is tilted such that the MUPUS penetrator will be in the field of view of the sensors if the lander balcony is pointing in the right direction. TM will thus provide the temperature at the very surface at the PEN location.

- ANC-T, a PT100 temperature sensor to monitor the local temperature at the final resting place of the anchor after it has been shot into the regolith of the comet nucleus. ANC-T provides an additional location for temperature measurement, laterally displaced by approximately 1 m from the MUPUS PEN sensors, and probably also at a greater depth. (It is likely that the deepest *in situ* measurements by PHILAE will be those of the anchor sensors.) A sufficiently high sampling rate in the first few minutes after deployment for ANC-T may yield constraints on the thermal diffusivity and conductivity of the cometary material (Paton, 2005).
- ANC-M, a miniature shock accelerometer (ISOTRON 2255B-1 from Endevco) monitoring the acceleration and deceleration of the anchoring projectile while it is fired into the ground.

The anchors will be accelerated pyrotechnically within a few milliseconds at the time immediately before lander touchdown to reach a launch speed of approximately $\sim$100 m s^{-1}. A peak acceleration value of about 90000 m s^{-2} (i.e. ca. 9000 g) is

Figure 10. Example of an anchor test shot. The target sample is a sintered CO_2 ice crust with softer material underneath. The shot holes and the anchor cables are visible.

expected. After a very short free flight period the anchor will penetrate the regolith and be decelerated by the resistance of the nucleus material. The main challenge concerning the selection of an appropriate accelerometer was the high dynamic range that it has to cover. On the one hand, ANC-M will have to survive the high amplitude acceleration phase and on the other hand it will have to be able to resolve a much smaller amplitude deceleration signal expected when the anchor will penetrate soft porous ice layers with low cohesion. With the 14-bit resolution of the flight unit and a sampling frequency of $\sim$50 kHz an accuracy of about 1.5 g can be achieved. The chosen sensor type thereby will allow to record the full acceleration phase (which is important for calibration purposes) while still giving a reasonable signal for sintered porous ices. Judging from comet analogue samples, a sintered water ice crust is to be expected for the nucleus of Comet Churyumov-Gerasimenko.

2.3.1. *Dynamic Penetrometry Tests with MUPUS ANC*

Penetrometry tests have been performed to check the performance of the anchoring harpoon and to calibrate the dynamic strength measurements. We show results of a shot into a CO_2 ice sample in Figures 10 and 11. Two shot holes are visible together with parts of the anchoring cables in Figures 10. At the impact sites, small craters with diameters larger than those of the penetration channels are visible. Note that the projectiles were accelerated with a cold gas system. The maximum acceleration in this experiment was lower than the acceleration expected for the PHILAE anchors.

In Figure 11 the deceleration profile measured by the shock accelerometer in one of the anchors is displayed together with a fit calculated with the similarity model described by Kömle *et al*. (2001). To calibrate the data in terms of strength/cohesion, a quasi-static strength measurement was performed close to the impact site. This measurement consisted of a slow (40 mm s^{-1}) penetration of a cylindrical rod

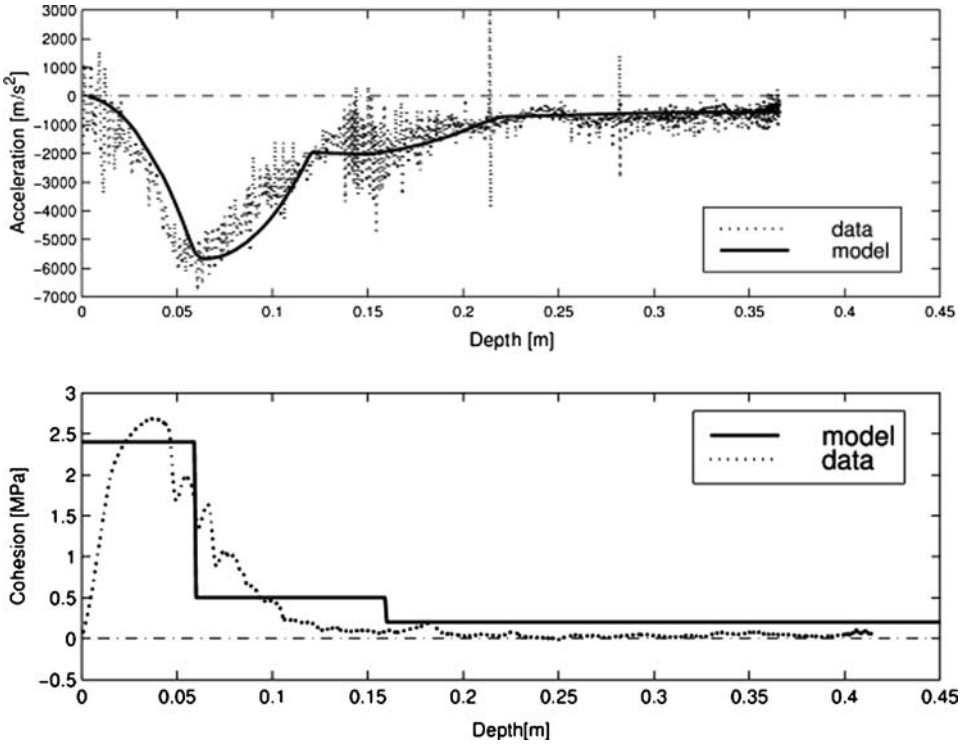

Figure 11. Upper panel: Accelerometer signal recorded from the impact close to the centre of the target. Lower panel: Strength profile obtained by an independent quasi-static measurement with a conventional force cell.

with a 60° tip into the sample, whereby the resistance force was measured by a conventional load cell that was mounted at the top of the rod. The results of the quasi-static measurements are shown in the lower panel, together with a simple fit to obtain a strength profile. The main vertical structure of the layer seen in the quasi-static test, namely a strong surface crust and a slightly consolidated part below, is also well represented in the deceleration data. This demonstrates that the dynamic penetrometry method, together with an appropriate model of the tip geometry, should be able to detect at least variations and discontinuities in the vertical strength profile. More detailed discussions of the penetrometry tests have been discussed by Kargl *et al*. (2001) and Kömle *et al*. (2001).

3. Resources

The following table gives an overview of the required resources. Considering the complex mechanics that are required to deploy and insert the penetrator, the overall

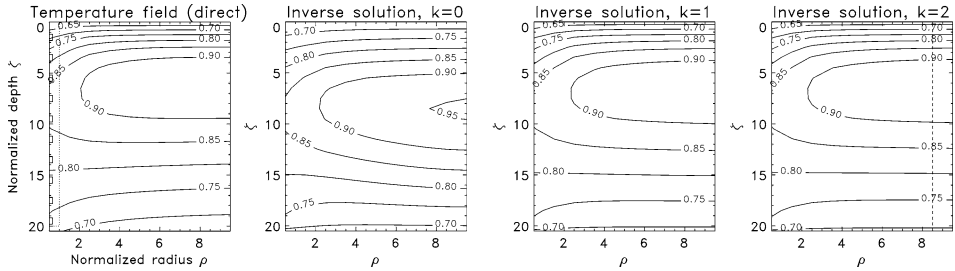

Figure 12. Direct ("true") temperature field (left, PEN marked with dotted lines and sensor locations marked by small rectangles) and "evolution" of the inverted temperature field with increasing order k of the solution in normalized coordinates. The dashed vertical line in the rightmost plot indicates the location of the estimate of the undisturbed profile.

experiment mass is very moderate. The data volume contains 2 Mbit of accelerometer data (sampled during anchor shots at the very beginning) and a very low data volume for the remaining science data (temperature and thermal properties data). If needed, the data rate can further be reduced by configuring larger time intervals between measurement scans. The average power consumption can only be estimated because it is partly determined by the heating power needed to keep the front-end electronics inside the operating range, and, thereby, dependent on the actual ambient conditions on the nucleus.

Mass (total)	2.35 kg
ID + PEN	0.65 kg
DD + DS	0.85 kg
Main electronics	0.6 kg
TM	0.12 kg
Harness	0.13 kg
Volume (envelope on balcony)	565 × 160 × 188 mm
Power (total)	2.2 W*
Main Electronics	1.2 W
PENEL	0.2 W
TM	0.2 W
Data rate	180 kBit/h[a]

[a] Average for nominal long-term operations (measurements every 20 sec)

4. Conclusions

The combination of MUPUS sensors will provide us with temperatures, thermal properties and cohesion data for the uppermost 32 cm of a comet nucleus as a

function of time. Using MUPUS data, we will be able to determine the energy balance at one location of the nucleus as it approaches the Sun, thereby gaining insight into the way comets work. A very important aspect of the MUPUS research is to observe changes of physical properties *in situ*, and determine the specific timescales of processes modifying cometary matter. Thermal and mechanical properties can be interpreted in terms of microstructure parameters of the ice, such as particles with variable texture, contact area between individual grains, and a chain-like particle structure which might be expected from a low-density material as snow (e.g., Keller and Spohn, 2002 and references therein). Having in mind that one of the main goals of the mission is the search for pristine material, thought to be a record of the formation of the solar system, it is of extraordinary importance to understand how much the material analysed by COSAC, PTOLEMY and APXS has been modified in the geological time record of the nucleus.

Acknowledgements

The authors, the MUPUS team, appreciate very much the co-operation with the whole lander team. Markus Thiel, Max-Planck-Institut für Extraterrestrik, Garching, is responsible for the design of the lander's anchors, and was always very cooperative when the integration of the MUPUS sensors and their tests were concerned. The MUPUS project and MUPUS team members are supported by various grants, some of which are: Marek Banaszkiewicz: Grant No 2 PO3C.009.12 p/05; Andrew Ball: PPARC (Particle Physics and Astronomy Research Council), The Austrian Academy of Sciences, and the Royal Society. German contribution: DLR grant WE 150 OH 9503 7-ZA. Austrian contribution: FWF Projects P12416 and P15470".

5. Appendix

The principles of temperature and thermal property measurements are very simple, but ensuring that the measured temperature is representative of the environment temperature can pose great difficulty. The very existence of any thermal probe influences the temperature field, and the MUPUS PEN too can have a significant influence on the sub-surface temperature field. If its thermal diffusivity is much larger than that of the ambient material, heat conduction through the penetrator rod can result in a distortion of the temperature gradient, resembling a thermal short circuit. This is a common effect of all heat flow experiments employing penetrators.

Especially in cases where measurement errors play a significant role, using forward modelling to explain the data is a way to pick one model that appears to be physically realistic, but this model is not necessarily the only one fitting the

data. Forward modelling techniques demonstrate the existence of a solution, but the problem of uniqueness of the solution remains unsolved.

The calculation of an unperturbed temperature profile from perturbed data with associated errors is a classical problem of inverse theory. It differs from the classical forward heat conduction problem in that it does not require boundary conditions, but solves for them. In the case of an inverse heat conduction problem, we have temperature histories at a number of points inside the volume and try to calculate the boundary conditions, which involves estimating the temperature throughout the whole volume (e.g. Stolz, 1960). Hagermann and Spohn (1999) have successfully developed a numerical inversion scheme to find the undisturbed temperature profile. Their algorithm uses the time-slope dependent extrapolation of measured temperature histories (Kurpisz, 1991). The algorithm approaches the undisturbed temperature profile by adding time-dependent extensions to a stationary solution.

In normalised cylindrical coordinates r and z and normalised time t, the temperature response R of the i-th temperature sensor equals the normalised temperature at the sensor location

$$R_i(t) = T(r, z, t). \tag{A.1}$$

With the time derivatives

$$R_i^{(k)}(t) = \frac{d^k R_i(t)}{dt^k}, k = 1, 2, ... \tag{A.2}$$

we can find the solution

$$T_j(t) = \sum_{k=0}^{K} \sum_{i=1}^{l} \psi_{ij}^{(k)} R_i^{(k)}(t), \tag{A.3}$$

where the $\psi_{ij}^{(k)}$ are recursive solutions of

$$\underline{\underline{H}} \cdot \psi_{ij}^{(k)} = \psi_{ij}^{(k-1)}. \tag{A.4}$$

$\underline{\underline{H}}$ is the linear system describing the thermal system of the penetrator and the surrounding material. Figure 12 shows how the result of the transient temperature field is constructed from a crude stationary solution. The method proved to be robust in most realistically conceivable scenarios (Hagermann and Spohn, 1999).

References

Ball, A. J., Gadomski, S., Banaszkiewicz, M., Spohn, T., Ahrens, T. J., Whyndham, M., *et al.*: 2001, *Planet. Space Sci.* **49**(9), 961.

Banaszkiewicz, M., Seiferlin, K., Spohn, T., Kargl, G., and Kömle, N.: 1997, *Rev Sci. Instrum.* **68**, 4184.

Benkhoff, J. and Spohn, T.: 1991, *Geophys. Res. Lett.* **18**, 261.

Benkhoff, J., *et al.*: 1995, SuSI Proposal (Principal Investigator: Dr. Johannes Benkhoff, Southwest Research Institute, San Antonio). SwRI Proposal No. 15-17876, May 1995.
Benkhoff, J. and Huebner, W. F.: 1995, *Icarus* **114**(2), 348.
Benkhoff, J., Seidensticker, K. J., Seiferlin, K., and Spohn, T.: 1995, *Planet. Space Sci.* **43**, 353.
Benkhoff, J.: 2002, *Adv. Space Res.* **29**(8), 1177.
Espinasse, S., Klinger, J., Ritz, C., and Schmitt, B.,1991, *Icarus* **92**, 350.
Grün, E., Heidrich, R., Hesselbarth, P., Kohl, H., and Benkhoff, J.: 1991, *Geophys. Res. Lett.* **18**, 257.
Grün, E., Bar-Nun, A., Benkhoff, J., Bischoff, A., Düren, H., Hellmann, H., *et al.*, 1991, in: Newburn, Jr., R. L., Neugebauer, M., and Rahe, J. (eds.), *Comets in the Post-Halley Era* (Kluwer Academic Publishers, Dordrecht), p. 277–297.
Hagermann, A.: 1996, Measurement of the subsurface temperature profile of a cometary nucleus: Model calculations for the PEN-TP experiment of the MUPUS package (in German). Diploma thesis, Institut für Planetologie, Westfälische Wilhelms-Unversität Münster.
Hagermann, A.: 1999, Die Ermittlung des oberflächennahen Temperaturfeldes aus einer gestörten Gradientenmessung. Zur Inversion planetarer Wärmeflußmessungen unter besonderer Berücksichtigung des Experiments MUPUS PEN-TP. Ph.D. thesis, Westfälische Wilhelms-Universität Münster.
Hagermann, A. and Spohn, T.: 1996, *Adv. Space Res.* **23**(7), 1333.
Huebner, W. F. and Benkhoff, J.: 1997, *Earth Moon Planets* **77**(3), 217.
Huebner, W. F. and Benkhoff, J.: 1999, *Space Sci. Rev.* **90**(1/2), 117
Kargl, G., Macher, W., Kömle, N. I., Thiel, M., Rohe, C., and Ball, A. J.: 2001, *Planet. Space Sci.* **49**(5), 425.
Keller, T. and Spohn, T.: 2002, *Planet. Space Sci.* **50**, 929.
Klinger, J.: 1981, *Icarus* **47**, 320.
Kofman, W., Herique, A., Goutail, J.-P., Hagfors, T., Nielsen, E., Barriot, J.-P., *et al.*: The comet nucleus sounding experiment by radiowave transmission (CONSERT); a short description of the instrument and of the commissioning stages, this issue.
Kömle, N. I., Ball, A. J., Kargl, G., Keller, T., Macher, W., Thiel, M., *et al.*: 2001, *Planet. Space Sci.* **49**(6), 575.
Kömle N. I.: 1997, *Planet. Space Sci.* **45**(12), 1515.
Kurpisz, K.: 1991, *J. Heat Transfer* **113**, 280.
Marczewski, W., Schröer, K., Seiferlin, K., Usowicz, B., Banaszkiewicz, M., Hlond, M., *et al.*: 2004, *J. Geophys. Res.* **109**(E7), 1.
Paton, M.: 2005, Penetrometry of NEOs and Other Solar System Bodies. Ph.D. thesis, The Open University.
Prialnik, D., Benkhoff. J., and Podolak, M.: 2004, in: Festou, M., Keller, H. U., and Weaver, H. A. (eds.), *Comets II* (University of Arizona Press, Tucson).
Seidensticker, K. J., Möhlmann, K. J. D., Apathy, I., Schmidt, W., Thiel, K., Arnold, W., *et al.*: *Space Sci. Rev.*, this issue, doi: 10.1007/s11214-006-9118-6.
Seiferlin, K., Spohn, T., and Benkhoff, J.: 1995, *Adv. Space Res.* **15**(10), 35.
Seiferlin, K., Hagermann, A., Banaszkiewicz, M., and Spohn, T.: 2001, in: Kömle, N. I., Kargl, G., Ball, A. J., Lorenz, R. D. (eds.), *Penetrometry in the Solar System* (Verlag der Österreichischen Akademie der Wissenschaften, Vienna).
Seweryn, K., Banaskiewicz, M., Grunwald, M., Grygorczuk, J., and Spohn, T.: *Int. J. Heat Mass Transf.* **48**, 3713.
Smoluchowski, R.: *J. Geophys. Res.* **87**, 422.
Spohn *et al.*: 1995, MUPUS Proposal (Responsible Proposer: Prof. Tilman Spohn, Institut für Planetologie, Westfälische Wilhelms-Universität, Münster), June 1995.
Spohn, T. and Benkhoff, J.: 1990, *Icarus* **87**, 358.
Steiner, G.: 1990, *Astron. Astrophys.* **240**, 533.

Steiner, G. and Kömle, N. I.: 1991, *Planet. Space Sci.* **39**, 507.

Steiner, G., Kömle, N. I., and Kührt, E.: 1991, in: Kömle, N. I., Bauer, S. J., and Spohn, T. (eds.), *Theoretical Modelling of Comet Simulation Experiments* (Austrian Academy of Sciences Press, Vienna).

Stolz, G.: 1960, *J. Heat Transfer* **82**, 20.

Thiel, M., Stöcker, J., Rohe, C., Hillenmaier, O., Kömle, N. I., and Kargl, G.: 2001, in: Kömle, N. I., Kargl, G., Ball, A. J., and Lorenz, R. D. (eds.), *Penetrometry in the Solar System* (Austrian Academy of Sciences Press, Vienna), p. 137–149.

Thiel, M., Stöcker, J. E., Rohé, C., Kömle, N. I., Kargl, G., Hillenmaier, O., *et al.*: 2003, in: Harris, R.A. (ed.), *10th European Space Mechanisms and Tribology Symposium*. ESA SP 524 (ESA Publications Division, Noordwijk), p. 239–254.

Thiel, M., Stöcker, J. E., Rohé, C., Kömle, N. I., Kargl, G., Hillenmaier, O., *et al.*: 2003, The ROSETTA Lander anchoring system. in: 10th European Space Mechanisms and Tribology Symposium. R.A. Harris (ed.). ESA SP 524, ESA Publications Division, Noordwijk, 239–254.